Hindawi
Geofluids
Volume 2022, Article ID 6413669, 15 pages
https://doi.org/10.1155/2022/6413669

Research Article

Study on Pressure Characteristics of Disturbed Wells due to Interwell Fracturing Interference and Its Application in Small Well Spacing Fracturing

Yanjun Zhang,[1,2] **Fan Lu**,[3] **Zhibo Guo**,[4] **Le Yan**,[1] **Tianlu Xu**,[5] **Hongkui Ge**,[2] **Shun Liu**,[1] **and Desheng Zhou**[1]

[1]*College of Petroleum Engineering, Xi'an Shiyou University, Xi'an, Shanxi 710065, China*
[2]*State Key Laboratory of Petroleum Resources and Prospecting, China University of Petroleum at Beijing, Beijing 102249, China*
[3]*No.5 Oil Production Plant, Changqing Oilfield Company, Xi'an, Shaanxi 710021, China*
[4]*No.1 Oil Production Plant, Changqing Oilfield Company, Xi'an, Shaanxi 710021, China*
[5]*Jiqing Oilfield Region, PetroChina Xinjiang Oilfield Company, Jimusar, Xinjiang 831700, China*

Correspondence should be addressed to Yanjun Zhang; 2017310209@student.cup.edu.cn

Received 31 January 2022; Accepted 7 April 2022; Published 26 April 2022

Academic Editor: Jin Qian

In order to maximize the production of unconventional oil and gas reservoirs, the well spacing has been shrinking continuously. Thus, the interwell fracturing interference usually occurs, which brings some problems affecting the fracturing efficiency. As one of the most challenging issues, a set of efficient methods for diagnosing wellhead pressure characteristics of interwell fracturing interference need to be established. In this study, taking the shale oil well platform of Lucaogou Formation as an example, the wellhead pressure resulted from interwell fracturing interference was analyzed. A real-time diagnosis method for each fractured stage based on the power-law model was proposed; the interference was further classified into four types. Meanwhile, the parameters of well spacing and completion were optimized. The results show that the power-law model of nonuniform pressure transmission in complex fracture networks is applicable for the evaluation of wellhead pressure fluctuation in real time. According to the differential pressure, the differential pressure derivative and the variation range of pressure interference during fracturing (PIF) and the interwell fracturing interference of Lucaogou Formation shale oil can be classified into pressure communication type (I), hydraulic fractures connected type (II), large natural fractures interconnected type (III), and composite type (IV). Specifically, the type of III and IV will do harm to the production, while the type of I is conducive to supplementing formation energy. The type of II may be conducive to supplementing formation energy in some situations. The well spacing of shale oil in the Lucaogou Formation is preferably 150~200 m, and the injection rate is optimized to 12 m^3/min. The findings of this study can help for better understanding of identifying wellhead pressure characteristics of interwell fracturing interference and optimizing well spacing and completion parameters.

1. Introduction

The optimization of well spacing is an essential procedure in the development of unconventional oil and gas reservoirs. Reasonable well spacing contributes to enhancing oil recovery and reducing the adverse effect of interwell interference on production [1–6]. Interwell interference in conventional reservoirs is dominated by pore pressure disturbance in matrix during production, while the main reason of interwell fracturing interference is connected fractures in unconventional reservoirs. Since the well spacing in unconventional reservoirs is continuously narrowed during multistage fracturing, the interwell fracturing interference caused by the communication of fractures has become a prominent issue [7–9], which influences the efficiency of fracturing and does harm to the recovery of oil and gas [10–13].

The interwell fracturing interference can be divided into two types including pressure communication and fracture

connection [14–16]. Fractures in disturbed wells are activated by the fluctuating pressure that significantly increases in a short period.

The slight interwell pressure interference because of microfracture is regarded as the pressure communication [17]. The type of fracture connection interference is also called fracture hit, which is mainly caused by the connection of asymmetric volume fractures formed in fracturing wells and disturbed wells [18]. The change of stress field during fracturing affects the fracture hit, while the distribution of fracturing fluids and proppants also plays an important role [19, 20]. Results indicate that the existence of the pressure hit accelerates the balance of bottom hole pressure based on the embedded discrete fracture model (EDFM) [21]. Besides, the pressure response during shut-in can be simulated by an analytical model that considers fracture hit [22]. Current publications have focused on the influence of the fracture propagation on interwell interference. However, the requirements needed to reduce negative effects of interwell fracturing interference have not been satisfied by roughly dividing the interference into pressure communication and fracture connection. In general, up to now, it is unclear on the wellhead pressure characteristics. There is still no reasonable diagnosis method for analyzing wellhead pressure characteristics of interwell fracturing interference.

Conventional diagnosis methods for interwell interference include chemical liquid tracing, radioactive proppants tracing, and pressure interference tests. Affected by irregular fractures, the real-time tracking analysis of chemical liquid tracing is usually inaccurate. The radioactive proppants tracing is costly, and it is also difficult to obtain the fracture connection properties during production [23–25]. The pressure interference testing is a method that identifies the interwell interference by the pressure change of a monitoring well. It is low cost and can achieve real-time monitoring, but it has high requirements for the pressure data acquisition system in the monitoring well [26]. In our study, the pressure data acquisition during the fracturing of Jimsar shale oil is achieved by wellhead manometers. And the wellhead pressure fluctuation during shut-in is the only information that can be used to identify the interwell fracturing interference in time.

For unconventional reservoirs, some methods that reversely demonstrate the flow information of fracturing fluids by its regular change in pressure or flow rate have been developed in recent years, such as RTA (rate-transient analysis) technology. It was established based on the theory of linear stream and used for analyzing and identifying the flow state. While the field data indicate that the flow of fluids in complex fracture systems is more in accordance with power-law characteristics [27], fracture networks with strong heterogeneity are a crucial reason leading to this difference [28, 29]. The heterogeneous transmission of pressure results from the heterogeneity of fracture systems and the transmission follows the power-law characteristics [30]. Besides, the flow conductivity and drainage of complex fractures show the characteristics of the power-law [31]. The data analysis method for interwell fracturing interference is based on the power-law theory. It can be used to explain the flowing characteristics and predict the production performance of reservoirs when the interwell fracturing interference exits [32]. There is a precedent for applying the power-law model to the analysis of interwell fracturing interference. Although the strong heterogeneity of reservoirs is taken into consideration, most analyses are only applied during production.

Given the geological information, the fracturing parameters, and the pressure fluctuation phenomenon during fracturing of Jimsar shale oil, a diagnosis method for interwell fracturing interference based on the power-law model was put forward. The regularity of interwell interference was analyzed, and the interference was classified into four types. Meanwhile, the parameters of well spacing and completion were optimized. The study has constructive significance for quickly identifying wellhead pressure characteristics of the interwell fracturing interference and optimizing the well spacing and completion parameters.

2. Basic Description of Interwell Fracturing Interference

2.1. Geological Information. Jimsar Sag is located in the eastern part of Junggar Basin, with a structure of monocline low in the west and high in the east [33–35]. The shale oil is mainly produced from the Middle Permian Lucaogou Formation, as shown in Figure 1(a). The stratum of Lucaogou Formation belongs to lacustrine sediments with a clay mineral content of no more than 5% and relatively low water sensitivity [36]. The study area has relatively strong heterogeneity and a high formation pressure coefficient of 1.3, which is an abnormally high-pressure pressure system. The formation pressure is 39 MPa, and the temperature is 86°C [37].

2.2. The Fracturing Parameters of Target Wells. Multistage fracturing is commonly used for developing tight reservoirs, and the drillable bridge plug stage fracturing is widely applied [38, 39]. To achieve the high-efficient development of Lucaogou Formation shale oil, an LCG well platform was designed, and the combination of long horizontal well and intensive cutting was used. The target wells are, respectively, numbered as LCG-1, LCG-2, LCG-3, LCG-4, and LCG-5. The relative position of wells is shown in Figure 1(b). The distance between wells LCG-1, LCG-2, and LCG-3 is 200 m, and the distance between wells LCG-4 and LCG-5 is 300 m.

Wells in the research area generally have a well depth in a range of 3900~4400 m, with a vertical depth of around 2700 m, a stimulation section length of about 1400 m, an average cluster distance of approximately 15 m, and a maximum injection rate of $14 m^3$/min. The detailed parameters are shown in Table 1. The length of the stimulation length of wells LCG-1, LCG-2, LCG-3, LCG-4, and LCG-5 is 1338 m, 1502 m, 1494 m, 1420 m, and 1330 m, respectively. The number of fracturing segments is, respectively, 30, 30, 33, 26, and 27, respectively. The reasonable design of parameters, such as the maximum injection rate, total injection amounts, and the injection rate, can realize the accuracy control of the fracturing scale of reservoirs. Meanwhile, these

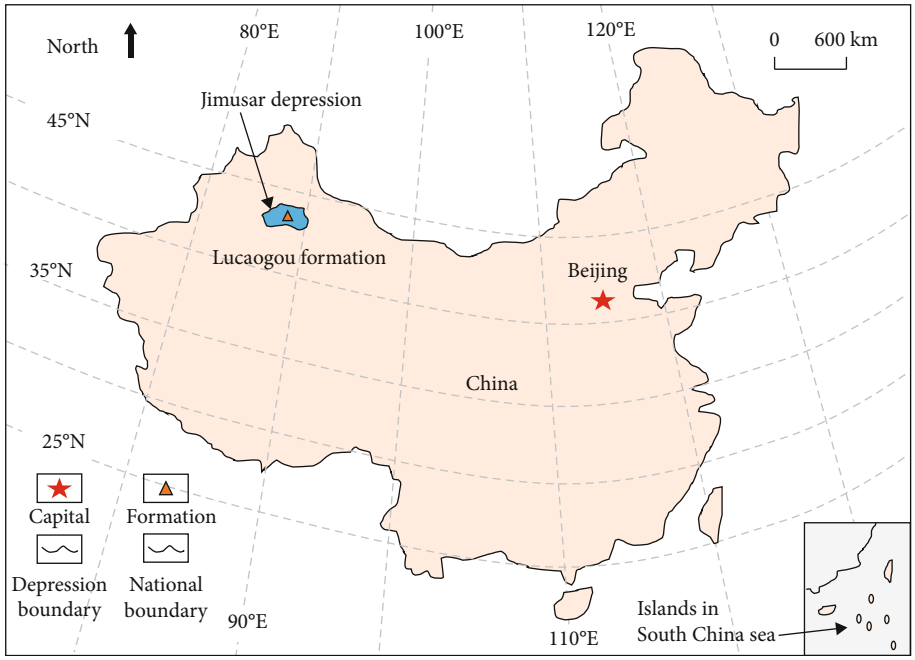

(a) The location of the study area

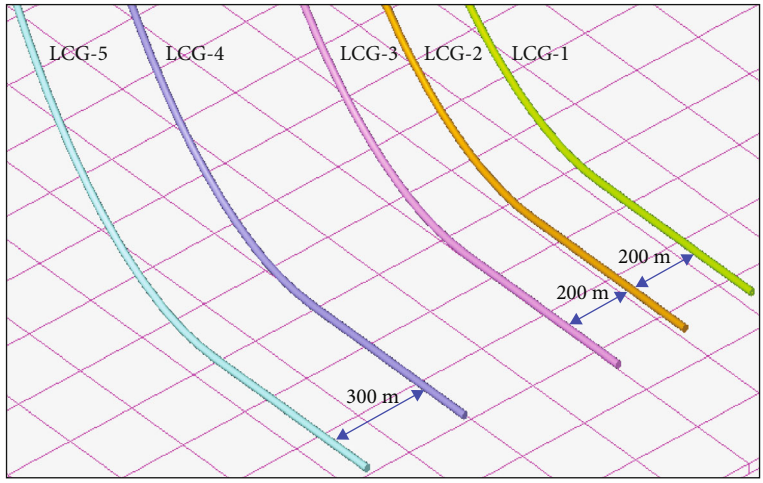

(b) The relative position of wells

Figure 1: The description of study location and well relative position.

Table 1: Well depth, length of horizontal segments, and fracturing parameters.

Well number	Well depth/m	True vertical depth/m	Length of reformation segments/m	Numbers of fracturing segments	Average cluster distance/m	Maximum injection rate (m^3/min)
LCG-1	3978.2	2655.7	1338	30	15.5	13.5
LCG-2	4310	2694	1502	30	15.2	14
LCG-3	4346	2704.9	1494	33	15.2	14
LCG-4	4190	2714.14	1420	26	15.5	13
LCG-5	4168	2727.07	1330	27	15.3	14

parameters are significant indicators that affect the degree of interwell fracturing interference [40].

As shown in Figure 2, when fracturing the main well, the disturbed wells are in post-frac shut-in, and its wellhead pressure decreases gradually. When fracturing well LCG-4, the wellhead pressure of well LCG-5 that has been fractured increases. When fracturing well LCG-2, pressure fluctuation appears in the wellhead of the fractured well LCG-1. When

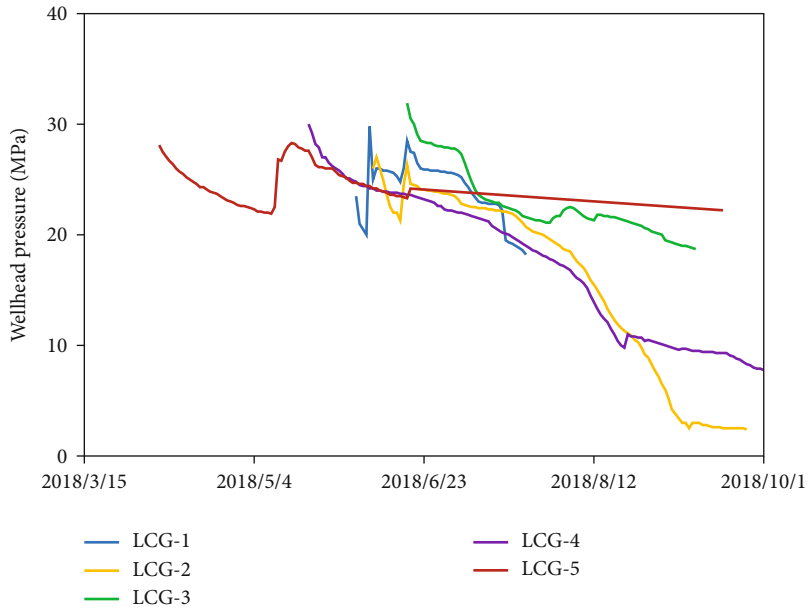

Figure 2: Variation of wellhead pressure of disturbed wells when they are in shut-in.

fracturing well LCG-3, the wellhead pressure of both wells LCG-2 and LCG-1 increases sharply. For data collection reasons, the change of pressure in well LCG-1 is recorded incompletely when well LCG-3 is fractured. Since well LCG-1 is interfered with by well LCG-2, well LCG-2 is interfered with by well LCG-3, and well LCG-5 is interfered with by LCG-4, the pressure interference characteristics of wells interfered with each other of the above three groups are mainly analyzed.

2.3. The Existed Problems. For the interwell fracturing interference of Jimsar shale oil, the following problems existed in the analysis. (1) The pressure acquisition is achieved by wellhead manometers, and compared to the accurate bottom hole pressure (BHP), the pressure interference response reflected by the wellhead pressure shows poor sensitivity. However, wellhead pressure is the only effective information capable of identifying the interwell fracturing interference. (2) The development of Jimsar shale oil is generally performed by processes of post-fracturing shut-in (i.e., no well opening after fracturing). In shut-in, the fluid in the wellbore is mainly fracturing fluid that does not flow back, and the influence of wellbore on wellhead pressure is small due to the relatively low dissolved gas-oil ratio in the original formation. (3) The pressure in complex fracture systems during shut-in is in an unbalanced state. With microfractures to be filled with liquid and the filtration loss of the matrix, traditional well testing theory cannot be used to reasonably explain the wellhead pressure data. Additionally, the cost of well testing later is high, and performing well testing will take a long time, which makes the requirements for timely adjusting fracturing parameters and quickly pre-judging interference that may appear cannot be satisfied. Therefore, the interwell communication in Jimsar drives the study on interwell interference toward an idea of accurate diagnosis of each fractured stage. In this way, the identification of interwell fracturing interference characteristics can be realized with the wellhead pressure data.

3. A Diagnosis Method for Interwell Fracturing Interference

Compared with conventional reservoirs that apply hydraulic fracturing, complex fracture networks are generally formed in tight reservoirs that adopt multistage fracturing. There are many problems when a method for evaluating the interwell interference in conventional reservoirs is used to analyze the interwell fracturing interference in unconventional reservoirs. For example, pressure transmission in heterogeneous fracture networks is not considered. The field data indicate that the power-law model including the nonuniform pressure transmission in heterogeneous systems is more suitable for analyzing the interwell interference during multistage fracturing in tight reservoirs [27]. Therefore, a real-time diagnosis method for each fractured stage based on the power-law model is established.

3.1. Theoretical Basis. Under complex geological conditions, the instantaneous pressure transmission in heterogeneous fracture systems does not follow Darcy's law very well, while the power-law model can better describe the characteristics of pressure change over time and space [28–30]. The expression of flux law is as follows:

$$v(x,t) = -\lambda_{\alpha,\beta} \frac{\partial^{1-\alpha}}{\partial t^{1-\alpha}} \left[\frac{\partial^{\beta}}{\partial x^{\beta}} p(x,t) \right], \tag{1}$$

where x is distance, t is time, and $P(x,t)$ is pressure. All of $\lambda_{\alpha,\beta} = k_{\alpha,\beta}/\mu$, α, and β are less than 1. $\partial^{\alpha} f(t)/\partial t^{\alpha}$ is time

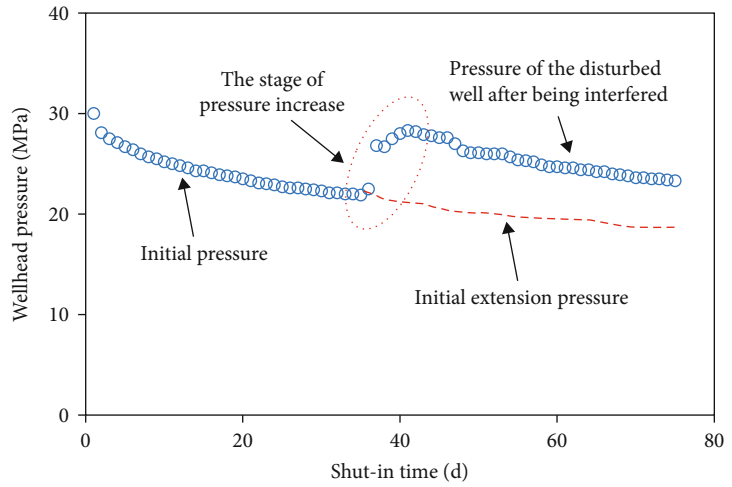

Figure 3: The schematic of the differential pressure calculation.

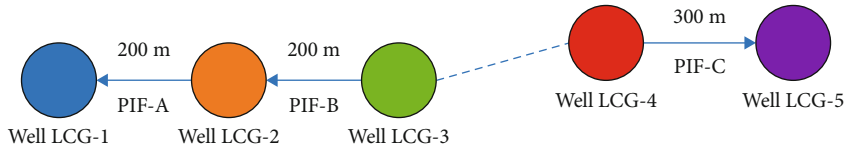

Figure 4: PIF diagram of interwell fracturing interference.

fractional derivative, and $\partial^{\beta} f(x)/\partial x^{\beta}$ is spatial fractional derivative, which, respectively, can be expressed as

$$\frac{\partial^{\alpha}}{\partial t^{\alpha}} f(t) = \frac{1}{\Gamma(1-\alpha)} \int_0^t dt' \left(t - t'\right)^{-\alpha} \frac{\partial}{\partial t} f\left(t'\right), \tag{2}$$

$$\frac{\partial^{\beta}}{\partial x^{\beta}} f(x) = \frac{1}{\Gamma(1-\beta)} \int_0^x dx' \left(x - x'\right)^{-\beta} \frac{\partial}{\partial x'} f\left(x'\right). \tag{3}$$

When performing production at a constant rate, the general solution of Equation (1) is obtained by Equations (2) and (3):

$$\bar{p}_D(x_D, s) = \frac{\pi}{2} \left(\frac{\eta\%}{L^{\beta+1}}\right)^{\frac{1-\alpha}{\alpha}} \frac{1}{s^{2-\alpha}} \left[\frac{1}{\beta/u^{\beta+1}} E_{\beta+1}\left(u x_D^{\beta+1}\right) - x_D^{\beta} E_{\beta+1,\beta+1}\left(u x_D^{\beta+1}\right)\right], \tag{4}$$

where $E_{\alpha,\beta}(x)$ is two-parameter Mittag-Leffler function, and when $X_D = 0$, the solution of Equation (4) is

$$p_D = (x_D = 0, t_D) = \frac{\pi}{2} \frac{t_D^{\alpha(\beta+1)}}{\Gamma(2 - \alpha/\beta + 1)}. \tag{5}$$

When the index is $a = \beta + 1 - \alpha/(\beta + 1)$, we can get $\Delta p \approx \Delta t$. When $\beta = 1$, the solution of $p_D(x_D, t_D)$ obtained is

$$p_D(x_D, t_D) = \frac{\pi}{2} t_D^{\frac{2-\alpha}{2\alpha}} H_{1,0}^{1,1}\left[\frac{x_D}{\sqrt{t_D}}\Bigg|_{(0,1)}^{\left(2-\frac{\alpha}{2}\right)\alpha}\right], \tag{6}$$

where $H_{p,q}^{m,n}\left[x\middle|_{(b_1,B_1),\cdots,(b_q,B_q)}^{(a_1,A_1),\cdots,(a_p,A_p)}\right]$ is H function and the differential pressure index in interfered wells is consistent with that in interference wells. Based on this, a method for pressure with power-law transmission characteristics is established to analyze the interwell fracturing interference.

3.2. The Establishment of the Method. Nonuniform pressure transmission has obvious power-law characteristics. As shown in Figure 3, the differential pressure $\triangle P$ specified in this study is a difference value between the real-time pressure of disturbed wells after being interfered by the fracturing well and its initial pressure trend, as shown in the following equation:

$$\triangle P = P_r - P_t, \tag{7}$$

where P_r is the real-time pressure after fracturing interference and P_t is the initial extension pressure. The wellhead pressure of disturbed wells continuously decreases during shut-in, which results from the filtration loss of fracturing fluid into the formation and an initial pressure imbalance in fracture systems. The initial extension pressure means that the fracturing fluid continuously leaks into the matrix and fractures during the disturbed wells being interfered,

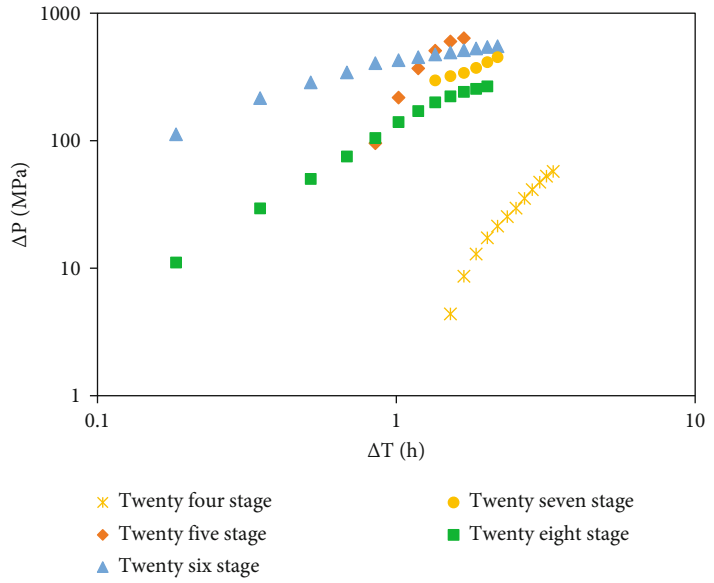

(a) ΔP

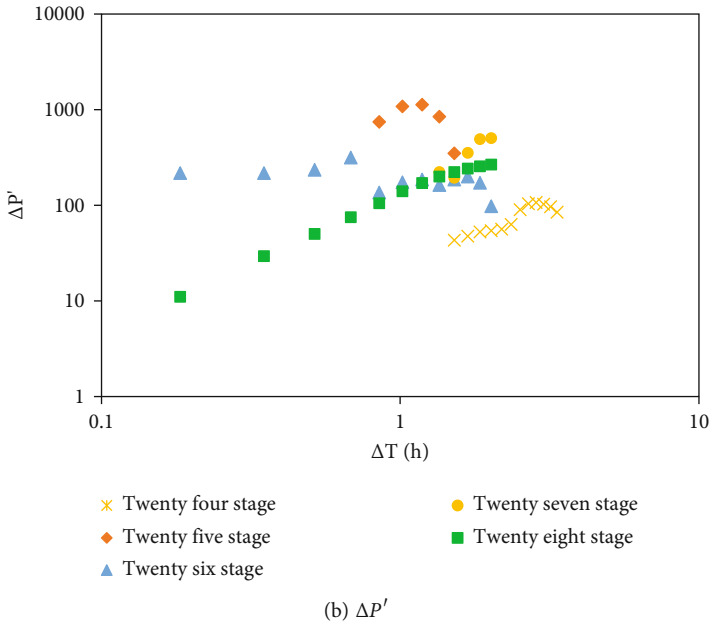

(b) $\Delta P'$

Figure 5: Continued.

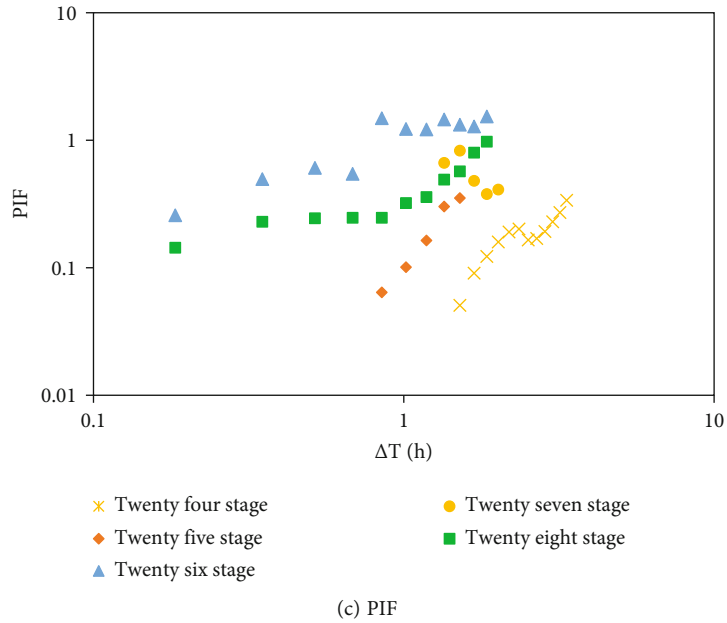

(c) PIF

Figure 5: The ΔP, $\Delta P'$, and PIF for each stage. Well LCG-1 is interfered with by well LCG-2 fractured at stages 24, 25, 26, 27, and 28.

and $\triangle P$ represents the pressure in the connection area between the two wells.

The magnitude of pressure interference (MPI) is used to evaluate the pressure interference degree [27]. And PIF specified herein is the pressure interference during fracturing, as shown in Figure 4. What is noteworthy is that general MPI may include the interference during drilling, fracturing, or producing of wells, while PIF in this study refers in particular to the pressure interference during multistage fracturing in unconventional reservoirs. The calculation equations are as follows:

$$\mathrm{PIF} = \frac{\triangle P}{2\triangle P'}, \tag{8}$$

$$\triangle P' = \frac{d\triangle P}{dlnt}, \tag{9}$$

PIF involves the $\triangle P$ and $\triangle P'$ of pressure change. In this way, the amplitude of pressure interference of disturbed wells interfered with by interference wells during fracturing can be obtained. Specific implementation steps are as follows: (a) acquiring $\triangle P$ and $\triangle P'$ by calculation according to Equations (7) and (9), plotting a relationship diagram showing the change of $\triangle P$ and $\triangle P'$ in a redouble logarithmic coordinate system, and preliminarily classifying the interwell interference by the tendency of $\triangle P$ and $\triangle P'$; (b) calculating PIF with the ratio relationship between $\triangle P$ and $\triangle P'$ according to Equation (8), and quantifying the interference level of fractures at all stages depending on the range of PIF, and further determining the type of interwell interference; and (c) preferably selecting the well spacing or completion parameters on the basis of PIF.

4. Real-Time Diagnosis of Interwell Fracturing Interference for Each Fractured Stage

Pressure testing is used as a direct means to analyze interwell fracturing interference level [26]. However, previous pressure testing mainly focuses on the interwell interference during production, while large multistage fracturing aims to produce fracture networks with high complexity. As a result, it is difficult to clearly explain the interwell fracturing interference by only using features of the production stage. Well LCG-1 is interfered with by well LCG-2, well LCG-2 is interfered with by well LCG-3, and well LCG-5 is interfered with by well LCG-4. The three groups of interference wells are analyzed based on the above diagnosis method for interwell fracturing interference established.

Well LCG-1 is interfered with by well LCG-2 fractured at stages 24, 25, 26, 27, and 28. As shown in Figure 5, the $\triangle P$, $\triangle P'$, and PIF at the above five stages are compared. It can be seen that all of the $\triangle P$, $\triangle P'$, and PIF of the interwell interference formed during fracturing at stage 24 are at a relatively low level; thus, the interwell interference formed at this stage is pressure communication dominated by microfractures. For well LCG-1, the respective $\triangle P$, $\triangle P'$, and PIF generated by interference during fracturing at stages 25, 26, and 27 have some differences. However, according to their variation range, the interference formed at these stages can be judged as the same type of interference, i.e., a pressure connection dominated by hydraulic fractures. And for well LCG-1, the $\triangle P$,$\triangle P'$, and PIF generated by interference during fracturing well LCG-2 at stage 28 are at a relatively high level. Thus, the interference at this stage may be the pressure interconnection dominated by natural fractures.

Well LCG-2 is interfered with well LCG-3 fractured at stages 6, 7, 8, and 9. As shown in Figure 6, the $\triangle P$, $\triangle P'$, and PIF generated in the adjacent well during fracturing at

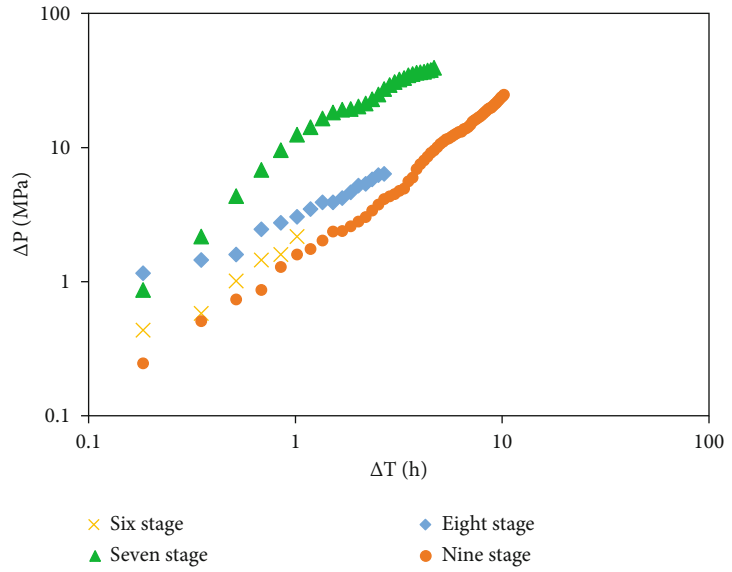

(a) $\triangle P$

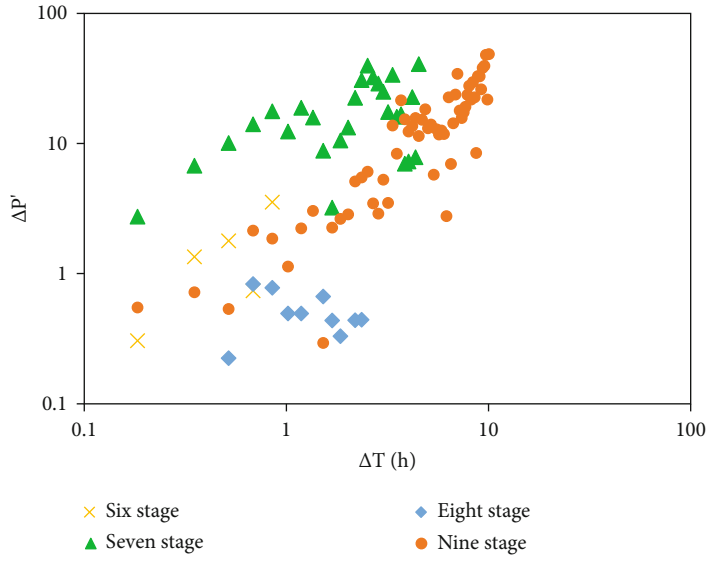

(b) $\triangle P'$

Figure 6: Continued.

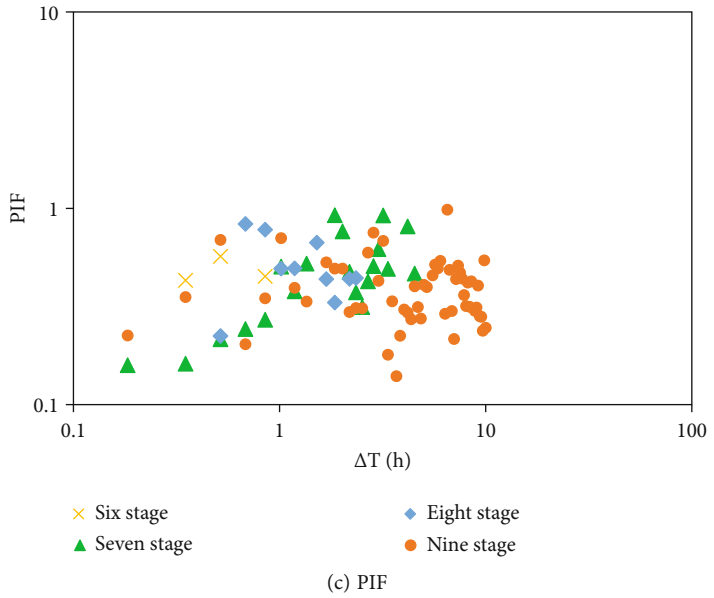

(c) PIF

Figure 6: The ΔP, $\Delta P'$, and PIF for each stage. Well LCG-2 is interfered with by well LCG-3 fractured at stages 6, 7, 8, and 9.

stage 7 are at a relatively high level, followed by those at stages 8, 6, and 9. The ranges of $\triangle P$, $\triangle P'$, and PIF show that the interference formed at stages 6, 7, 8, and 9 is of the same type, i.e., the interference dominated by the communication of hydraulic fractures. The difference of interference level at each stage may result from partially developed microfractures. The pressure disturbance formed by several microfractures during fracturing still can maintain a certain pressure after pressure release, which facilitates energy maintenance during the production of reservoirs.

Well LCG-5 is interfered with well LCG-4 when it was fractured at stages 19, 20, 22, 23, and 26. As shown in Figure 7, the $\triangle P$, $\triangle P'$, and PIF at stage 19 are at a relatively high level, but there is little difference for those at the other stages. The variation range of $\triangle P$, $\triangle P'$, and PIF indicates that the interference at stages 20, 22, 23, and 26 is of the same type. It can be regarded as the interference dominated by the connection of hydraulic fractures.

5. Discussion

5.1. Classification of Interwell Fracturing Interference of the Shale Oil Well Platform. Identifying the type of interwell fracturing interference will be helpful to understand the problems that may be brought by the interference, thus reducing the negative effect on production. Figure 8 shows the average value of PIF, a significant indicator of interwell interference level, calculated when wells LCG-1, LCG-2, and LCG-5 are fractured. Figure 8(a) shows that the average value of PIF of interference formed during fracturing at stage 24 is less than 0.4. It means that it is a pressure communication-typed interference with relatively low intensity dominated by microfractures. The average values of PIF at stages 25, 26, 27, and 28 are overall larger and in a range of 0.4~0.6. It means that the intensity of the interference is stronger than that at stage 24, and it is a hydraulic fracture communication-typed interference that may be accompanied by some microfractures. Figure 8(b) shows that the interference intensity during fracturing at stages 6, 7, 8, and 9 is similar, while the interference intensity at stage 9 is relatively weak. Therefore, the interference formed during fracturing at stages 6, 7, 8, and 9 is of the same type and is the interference dominated by the connection of fracturing fractures. Figure 8(c) shows that the PIF value during fracturing at stage 26 is 0.34, so the interference at this stage is of relatively low interference intensity and is the interference type dominated by microfractures. The PIF value during fracturing at stage 19 is larger, and the interference at this stage results from the communication of hydraulic and natural fractures. The PIF values at the other stages are in a range of 0.4-0.6, and the interference is the communication type dominated by hydraulic fractures and accompanied by developed microfractures.

The classification of interwell fracturing interference is shown in Table 2, including a pressure communication type, a hydraulic fractures connected type, a large natural fractures interconnected type, and a composite type. The pressure communication type, with a PIF in a range of 0~0.4, is mainly the communication of microfractures or branching fractures. The pressure rises slowly when fracturing fluid is filled, and the pressure has mild change during unloading, which is conducive to maintaining the pressure in reservoirs. The hydraulic fractures connected type, with a PIF in a range of 0.4~0.6, is mainly the connection of hydraulic fractures. The pressure rises fast when fracturing fluid is filled, and the response pressure is relatively sensitive during unloading. Moreover, if accompanied by more microfractures, it is conducive to pressure maintenance later. Large natural fractures interconnected type, with a PIF in a range of 0.6~1, is mainly the communication of large natural

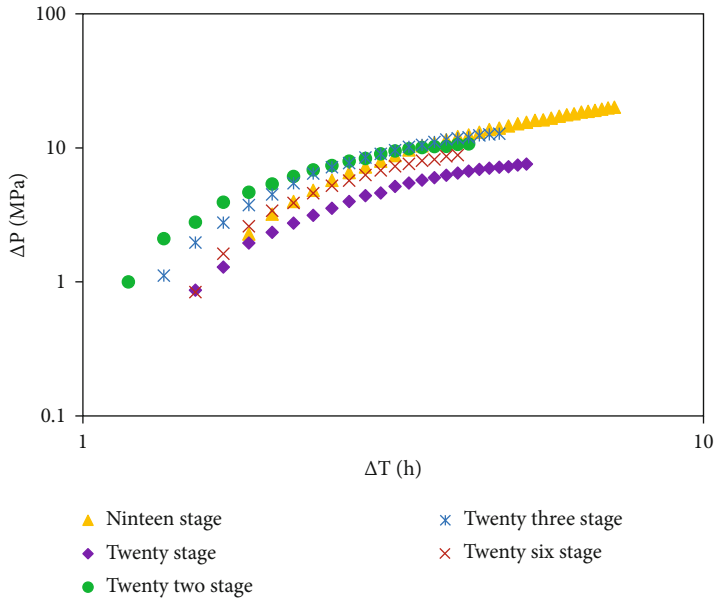

(a) $\triangle P$

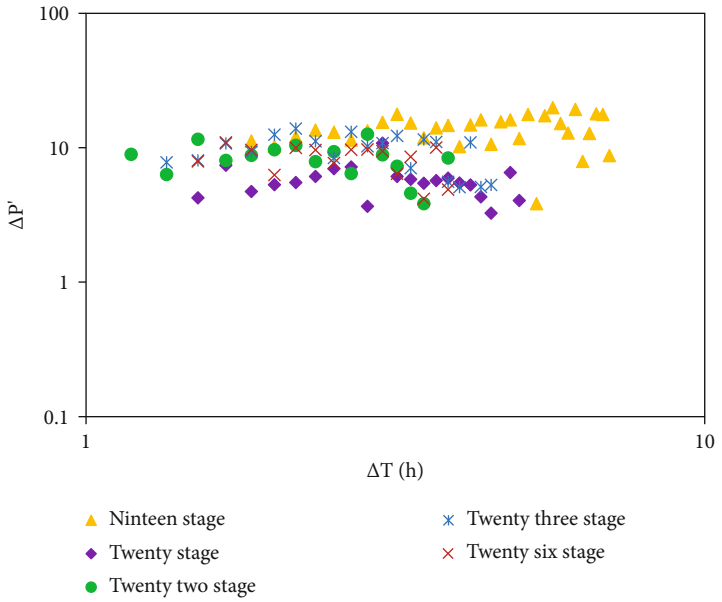

(b) $\triangle P'$

Figure 7: Continued.

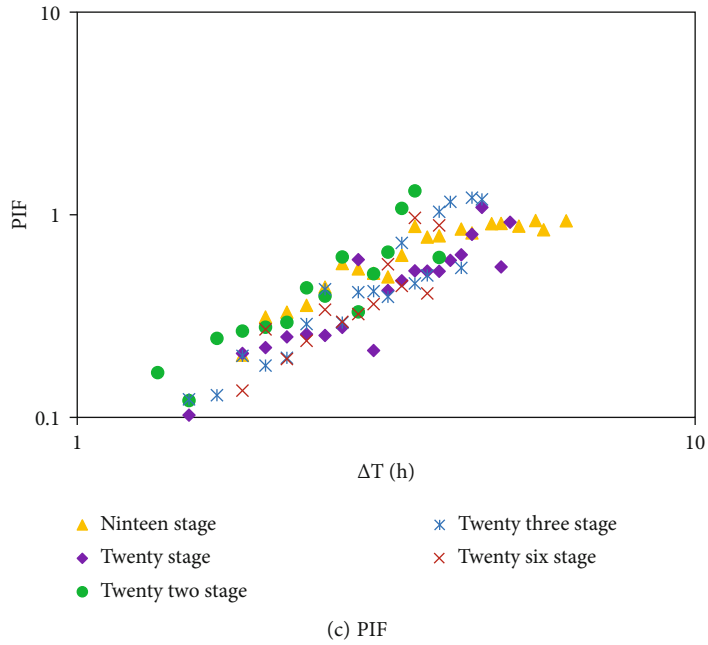

(c) PIF

Figure 7: The ΔP, $\Delta P'$, and PIF for each stage. Well LCG-5 is interfered with when well LCG-4 is fractured at stages 19, 20, 22, 23, and 26.

fractures or faults. The pressure rises fast when fracturing fluid is filled, the response pressure decreases slowly during unloading, and the pressure of the two wells is synchronized, which is bad for maintaining the pressure of reservoirs later. Underground fractures are often relatively complex. There is a situation that natural fractures are connected to hydraulic fractures, even including pressure communication. So this situation is defined as a composite type with a PIF value in a range of 0.6~1, which is characterized by the domination of large natural fractures interconnected. The pressure rises fast, and the response pressure decreases slowly during unloading. The pressure of the two wells is synchronized, and a large area of interference appears, which is not conducive to pressure maintenance later.

The LCG-5 well was fractured first, and then serious disturbance appears because of encountered natural fractures when the nineteenth stage of well LCG-4 is fractured. This phenomenon corresponds to the result diagnosed by using the PIF value. So it further illustrates the rationality of the diagnosis method for interwell fracturing interference based on the power-law model and also enhances the feasibility of the classification.

5.2. Optimization of Well Spacing and Completion Parameters. Smaller well spacing will result in a greater degree of negative interwell fracturing interference, which will affect the later production, while larger well spacing will reduce the producing degree of reservoirs. On the basis of interference type and interference level generated during fracturing of Jimsar shale oil, well spacing is optimized by PIF parameters, as shown in Figure 9. When well spacing is 200 m, the average value of PIF at each stage is about 0.45, and when well spacing is 300 m, the average value of PIF at each stage is about 0.43. It can be seen that the interference level reduces with the increase of well spacing, and the well spacing is optimized by linear fitting the interwell interference level and well spacing. As the interference type is ideal when the PIF value is in a range of 0.4~0.6 and the maximization of producing degree of reservoirs is taken into consideration, the reasonable well spacing in the present development area is around 150~200 m.

Both well LCG-1 and LCG-2 have a well spacing of 200 m, but the injection rates of them are, respectively, 13.5m^3/min and 14m^3/min. As shown in Figure 10, the relationship between PIF values and injection rate of well LCG-1 and well LCG-2 can be seen that the interwell interference level rises with the increase of injection rate. When the injection rate is about 12m^3/min, the PIF value is approximately 0.45, which conforms to the classification criteria favorable for later production wells.

As shown in Table 3, the well spacing between the disturbed wells LCG-1, LCG-2, and LCG-5 and their corresponding interference wells is, respectively, 200 m, 200 m, and 300 m. According to statistics, the maximum injection rate of well LCG-1 and well LCG-2 with the same well spacing increases from 13.5 m^3/min to 14 m^3/min, and the proportion of interference magnitudes increases by 3.7%. It should be noted that the maximum injection rate in the research area is a sensitive factor that affects the interwell interference intensity. In order to further enhance oil recovery, well spacing is preferably 150~200 m, and the maximum injection rate reduces by 20% to about 12m^3/min, which are similar to the results of well spacing and injection rate optimized based on PIF. In order to reduce the interwell interference level in infill wells, both Wolfcamp and Delaware basins also adopt a similar approach [19].

5.3. Limitations. The identification and diagnosis method for interwell fracturing interference is still in an exploratory stage, and the research in the current stage has the following

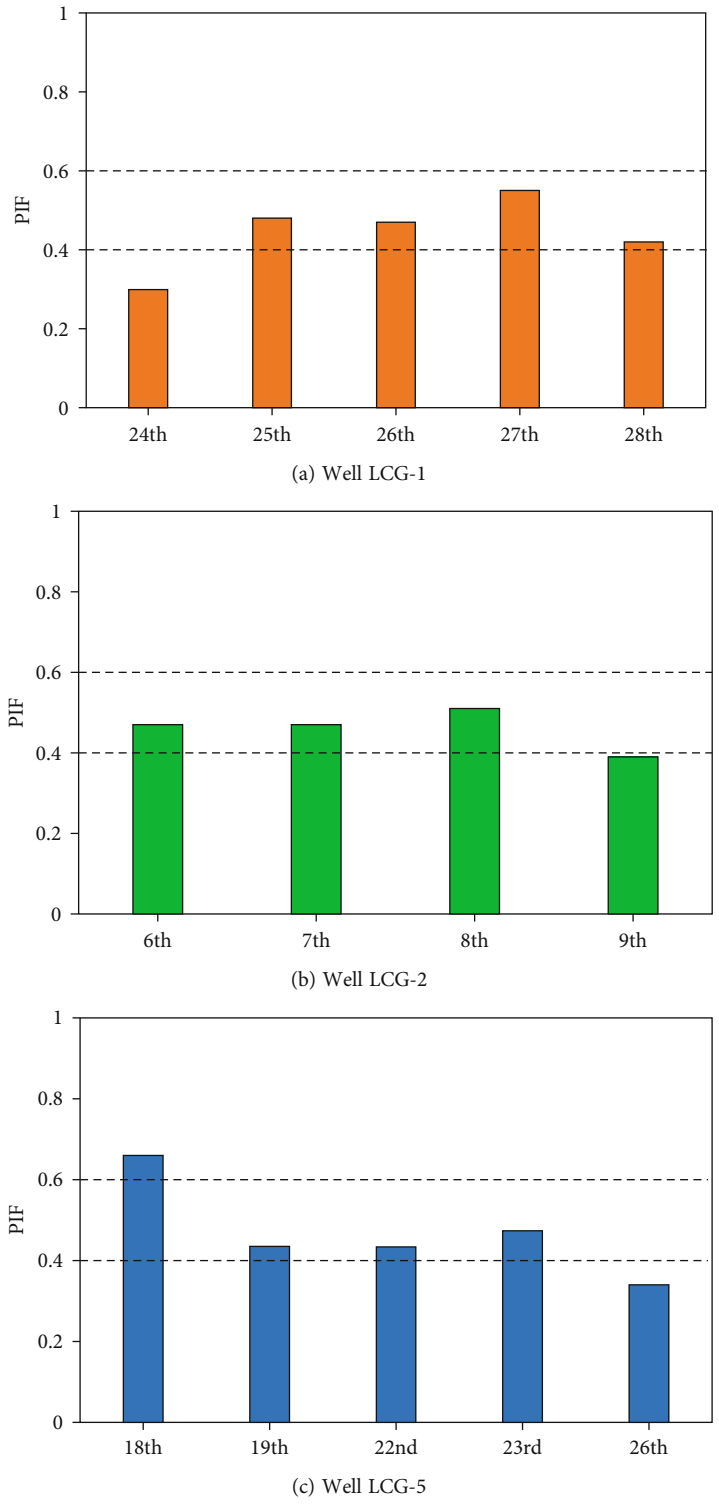

Figure 8: The PIF at each stage of LCG-1, LCG-2, and LCG-5.

limitations: (1) The wellbore in the process of post-frac shut in is filled with fracturing fluid, and its composition is relatively single. Thus, if the dissolved gas-oil ratio is relatively large after a long time of production, the relationship between the pressure in the wellbore and the bubble point pressure, as well as whether it is in a state of multiphase flow, should also be considered. (2) The real-time diagnosis method for each stage of interwell fracturing interference established herein is commonly applicable to identify the interwell interference during multistage fracturing. However, the specific parameters obtained have regional characteristics. Therefore, different oil fields can take these

Table 2: The type of interwell fracturing interference.

Label	Interference type	PIF	Communication media	Effect on production
I	Pressure communication	0~0.4	Micro- and branching fractures	Maintaining the pressure in reservoirs
II	Hydraulic fractures connection	0.4~0.6	Hydraulic fractures	Maybe be conducive to pressure maintenance
III	Large natural fractures connection	0.6~1	Natural fractures/faults	Bad for pressure maintenance
IV	Composite	0.6~1	Combination of above fractures	A large interference area and bad for pressure maintenance

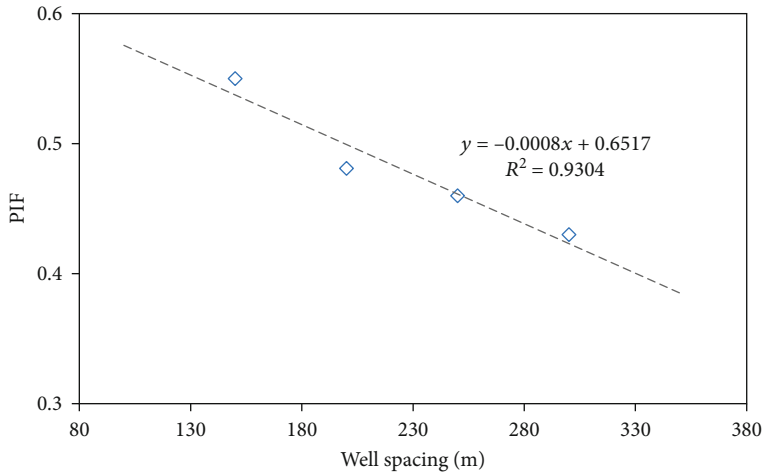

Figure 9: Preferable well spacing based on the PIF.

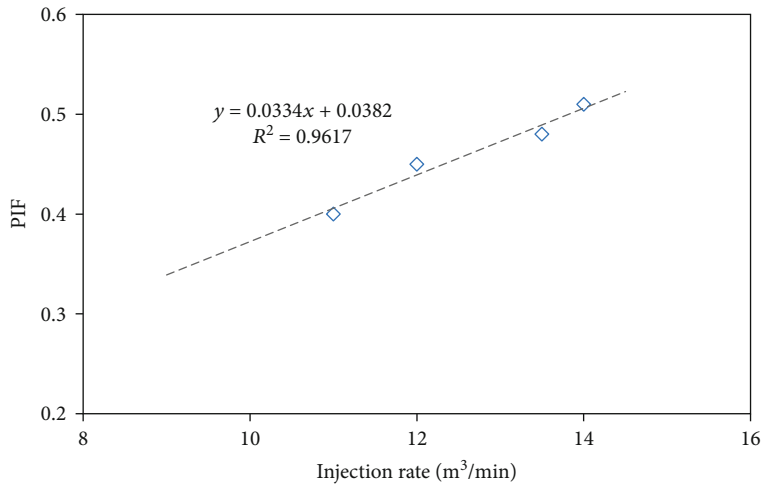

Figure 10: Preferable injection rate based on PIF.

Table 3: A table for preferable well spacing and injection rate.

Well number	Well spacing (m)	Maximum injection rate (m^3/min)	Proportion of interference magnitudes
LCG-1	200	13.5	10%
LCG-2	200	14	15%
LCG-5	300	14	30%

parameters as a reference since there must be some differences due to the complex geological environment and stimulation operation.

6. Conclusion

In this study, a diagnosis method for interwell fracturing interference based on the power-law model was put forward. The interwell fracturing interference was analyzed, and it

was classified into four types. Meanwhile, the parameters of well spacing and completion were optimized. The observations and conclusions are as follows.

(1) Aim to the current interwell fracturing interference of Jimsar shale oil, a real-time diagnosis method for each fractured stage based on the power-law model was proposed. In this method, the wellhead fluctuating pressure of adjacent wells was used, and the nonuniform pressure transmission in heterogeneous fracture systems was concerned

(2) The interwell fracturing interference can be classified into a pressure communication type (I), a hydraulic fractures connected type (II), a natural fractures interconnected type (III), and a composite type(IV), according to the range of PIF. Specifically, the type of III and IV will do harm to the production, while the type of I is conducive to supplementing energy. The type of II may be conducive to supplementing formation energy in some situations

(3) The level of interwell fracturing interference decreases with the increase of well spacing and rises with the increase of injection rate. In order to maximize the producing degree of Jimsar shale oil, the reasonable well spacing for the present development area is 150~200 m, and the reasonable fracturing injection rate is around $12 m^3$/min

Data Availability

Datasets related to this article can be found by connecting the corresponding author.

Conflicts of Interest

The authors declare that they have no conflict of interests.

Acknowledgments

This work was financially supported by the National Natural Science Foundation of China (Grant Nos. 51874242 and 51934005), the National Natural Science Foundation of China (Grant No. 52174032), the Strategic Cooperation Technology Projects of CNPC and CUPB (Grant No. ZLZX2020-01), and the Key Research and Development Program of Shanxi (Program No. 2021GY-112).

References

[1] W. A. N. G. Jing, Z. H. A. O. Wei, L. I. U. Huiqing et al., "Interwell interferences and their influencing factors during water flooding in fractured-vuggy carbonate reservoirs," *Petroleum Exploration and Development*, vol. 47, no. 5, pp. 1062–1073, 2020.

[2] F. Lalehrokh and J. Bouma, "Well spacing optimization in eagle ford," in *SPE/CSUR Unconventional Resources Conference–Canada*, Calgary, Alberta, Canada, September 2014.

[3] M. Baker, S. Mazumder, H. Sharma, J. A. Philpot, M. Scott, and R. Wittemeier, "Well design and well spacing optimisation in unconventional plays," in *SPE Asia Pacific Oil and Gas Conference and Exhibition*, Perth, Australia, October 2012.

[4] C. Aniemena, C. LaMarca, and A. Labryer, "Well spacing optimization in shale reservoirs using rate transient analytics.," in *Unconventional Resources Technology Conference (URTeC); Society of Exploration Geophysicists*, July 2019.

[5] E. Annan Boah, O. Kwami Senyo Kondo, A. Aidoo Borsah, and E. T. Brantson, "Critical evaluation of infill well placement and optimization of well spacing using the particle swarm algorithm," *Journal of Petroleum Exploration and Production Technology*, vol. 9, no. 4, pp. 3113–3133, 2019.

[6] R. S. Gurbanov, S. A. Musayeva, R. S. Gurbanov, and Z. M. Ahmedov, "Advanced well spacing system application in the development of oil and gas fields [J]," *Procedia Computer Science*, vol. 102, pp. 446–452, 2016.

[7] K. U. A. N. G. Lichun and L. I. Guoxin, "Considerations and suggestions on optimizing completion methods of continental shale oil in China," *Acta Petrolei Sinica*, vol. 41, no. 4, pp. 489–496, 2020.

[8] A. A. Awotunde, "Characterization of reservoir parameters using horizontal well interference test," in *SPE Annual Technical Conference and Exhibition*, San Antonio, Texas, USA, September 2006.

[9] M. Almasoodi, R. Vaidya, and Z. Reza, "Intra-well interference in tight oil reservoirs: what do we need to consider? Case study from the Meramec," in *Unconventional resources technology conference*, Denver, Colorado, USA,, July 2019.

[10] M. Meng, H. Ge, Y. Shen et al., "The effect of clay-swelling induced cracks on imbibition behavior of marine shale reservoirs," *Journal of Natural Gas Science and Engineering*, vol. 83, p. 103525, 2020.

[11] M. Meng, H. Ge, Y. Shen, L. Li, T. Tian, and J. Chao, "The effect of clay-swelling induced cracks on shale permeability during liquid imbibition and diffusion," *Journal of Natural Gas Science and Engineering*, vol. 83, p. 103514, 2020.

[12] X. Liang, F. Zhou, T. Liang, H. Su, S. Yuan, and Y. Li, "Impacts of pore structure and wettability on distribution of residual fossil hydrogen energy after imbibition," *International Journal of Hydrogen Energy*, vol. 45, no. 29, pp. 14779–14789, 2020.

[13] X. Liang, F. Zhou, T. Liang, Y. Huang, D. Wei, and S. Ma, "The effect of combined proppants upon the fracture conductivity in tight gas reservoirs," *Energy Reports*, vol. 6, pp. 879–884, 2020.

[14] A. Rangriz, R. J. Chalaturnyk, and D. Bearinger, "Deployment of pressure hit catalogues to optimize multi-stage hydraulic stimulation treatments and future re-fracturing designs of horizontal wells in Horn River Shale Basin," in *SPE Annual Technical Conference and Exhibition*, Calgary, Alberta, Canada, September 2019.

[15] R. Weijermars, "Optimization of fracture spacing and well spacing in Utica shale play using fast analytical flow-cell model (FCM) calibrated with numerical reservoir simulator," *Energies*, vol. 13, no. 24, p. 6736, 2020.

[16] W. Wu, J. Zhou, P. Kakkar, R. Russell, and M. M. Sharma, "An experimental study on conductivity of unpropped fractures in preserved shales," *SPE Production & Operations*, vol. 34, no. 2, pp. 280–296, 2019.

[17] A. Daneshy, J. Au-Yeung, T. Thompson, and D. Tymko, "Fracture shadowing: a direct method for determination of the reach and propagation pattern of hydraulic fractures in

horizontal wells," in *SPE Hydraulic Fracturing Technology Conference*, The Woodlands, Texas, USA, February 2012.

[18] S. Anusarn, J. Li, K. Wu et al., *Fracture hits analysis for parent-child well development*, American Rock Mechanics Association, 2019.

[19] P. Pankaj, "Decoding positives or negatives of fracture-hits: a geomechanical investigation of fracture-hits and its implications for well productivity and integrity," in *Unconventional Resources Technology Conference*, Houston, Texas, USA, July 2018.

[20] K. Zhao, X. Li, C. Yan, Y. Feng, L. Dou, and J. Li, "A new approach to evaluate fault-sliding potential with reservoir depletion," *SPE Journal*, vol. 24, no. 5, pp. 2320–2334, 2019.

[21] F. M. Xavier, Y. Wei, and G. Reza, "Modeling interwell interference due to complex fracture hits in eagle ford using EDFM," in *International Petroleum Technology Conference*, Beijing, China, 2019.

[22] X. Yang, W. Yu, K. Wu, and R. Weijermars, "Assessment of production interference level due to fracture hits using diagnostic charts," *Society of Petroleum Engineers.*, vol. 25, no. 6, pp. 2837–2852, 2020.

[23] A. Kumar and M. M. Sharma, "Diagnosing fracture-wellbore connectivity using chemical tracer flowback data," in *Unconventional Resources Technology Conference*, Houston,Texas, USA, 2018, August 9.

[24] M. Dawson and G. Kampfer, "Breakthrough in hydraulic fracture & proppant mapping: achieving increased precision with lower cost," in *Unconventional Resources Technology Conference*, San Antonio, Texas, USA, 2016, August 1.

[25] L. Cheng, N. Yang, and Z. Li, "Diagnosis and analysis of cross flow between layers," *Journal of the University of Petroleum, China (natural science edition)*, vol. 2, p. 50-52+56-5, 2002.

[26] A. Kumar, P. Seth, K. Shrivastava, R. Manchanda, and M. M. Sharma, "Integrated analysis of tracer and pressure-interference tests to identify well interference," *Society of Petroleum Engineers*, vol. 25, pp. 1623–1635, 2020.

[27] W. C. Chu, N. D. Pandya, R. W. Flumerfelt, and C. Chen, "Rate-transient analysis based on power-law behavior for Permian wells," *Society of Petroleum Engineers*, vol. 22, pp. 1360–1370, 2017.

[28] R. Raghavan and C. Chen, "Fractional diffusion in rocks produced by horizontal wells with multiple, transverse hydraulic fractures of finite conductivity [J]," *Journal of Petroleum Science & Engineering*, vol. 109, pp. 133–143, 2013.

[29] C. Chen and R. Raghavan, "Transient flow in a linear reservoir for space-time fractional diffusion [J]," *Journal of Petroleum ence & Engineering*, vol. 128, pp. 194–202, 2015.

[30] R. Raghavan, C. Chen, and J. DaCunha, "Nonlocal diffusion in fractured rocks," *Society of Petroleum Engineers.*, vol. 20, pp. 383–393, 2017.

[31] J. A. Acuña, "Analytical pressure and rate transient models for analysis of complex fracture networks in tight reservoirs," *Unconventional resources technology conference*, 2016.

[32] W.-C. Chu, K. D. Scott, R. Flumerfelt, C. Chen, and M. D. Zuber, "A new technique for quantifying pressure interference in fractured horizontal shale wells," *Society of Petroleum Engineers.*, vol. 23, no. 1, pp. 143–157, 2020.

[33] Z. Cao, G. Liu, Y. Kong et al., "Lacustrine tight oil accumulation characteristics: Permian Lucaogou Formation in Jimusaer Sag, Junggar Basin [J]," *International Journal of Coal Geology*, vol. 153, pp. 37–51, 2016.

[34] L. Hou, X. Luo, Z. Zhao, and L. Zhang, "Identification of oil produced from shale and tight reservoirs in the Permian Lucaogou shale sequence, Jimsar sag, Junggar Basin, NW China," *ACS Omega*, vol. 6, no. 3, pp. 2127–2142, 2021.

[35] Y. Su, M. Zha, X. Ding et al., "Pore type and pore size distribution of tight reservoirs in the Permian Lucaogou Formation of the Jimsar Sag, Junggar Basin, NW China [J]," *Marine and Petroleum Geology*, vol. 89, pp. 761–774, 2018.

[36] L. Kuang, T. A. N. G. Yong, L. E. I. Dewen et al., "Formation conditions and exploration potential of tight oil in the Permian saline lacustrine dolomitic rock, Junggar Basin, NW China," *Petroleum Exploration and Development*, vol. 39, no. 6, pp. 700–711, 2012.

[37] H. Pang, X. Q. Pang, L. Dong, and X. Zhao, "Factors impacting on oil retention in lacustrine shale: Permian Lucaogou Formation in Jimusaer Depression, Junggar Basin," *Journal of Petroleum Science and Engineering*, vol. 163, pp. 79–90, 2018.

[38] Q. Feng, S. Xu, and G. Ren, "Hierarchical optimization of well pattern parameters in multi-stage fractured horizontal well for tight oil [J]," *Acta Petrolei Sinica*, vol. 40, no. 7, pp. 830–838, 2019.

[39] R. Yong, C. Chang, D. Zhang et al., "Optimization of shale-gas horizontal well spacing based on geology-engineering-economy integration: a case study of well block Ning 209 in the national shale gas development demonstration area [J]," *Natural Gas Industry*, vol. 40, no. 7, pp. 42–48, 2020.

[40] R. Malpani, F. Alimahomed, C. Defeu et al., *Multigeneration section development in the Wolfcamp, Delaware Basin*, Unconventional resources technology conference, 2019.